Composites: Part A 43 (2012) 1561–1568

Contents lists available at SciVerse ScienceDirect

Composites: Part A

journal homepage: www.elsevier.com/locate/compositesa

Resistance to time-dependent deformation of polystyrene/carbon nanotube composites under cyclic tension

Yu Jia [a,b], Zhimin Jiang [b], Jinping Peng [b], Xinglong Gong [a,*], Zhong Zhang [b,c,*]

[a] CAS Key Laboratory of Mechanical Behavior and Design of Materials, Department of Modern Mechanics, University of Science and Technology of China, Hefei 230027, China
[b] National Center for Nanoscience and Technology, Beijing 100190, China
[c] Center for Nano and Micro Mechanics, Tsinghua University, Beijing 100084, China

ARTICLE INFO

Article history:
Received 11 February 2012
Received in revised form 10 April 2012
Accepted 14 April 2012
Available online 22 April 2012

Keywords:
A. Polymer–matrix composites (PMCs)
B. Creep
D. Electron microscopy
E. Extrusion

ABSTRACT

Materials subject to cyclic stress can succumb to fatigue, causing failure at stress levels much lower than those in static loading cases. Herein we discussed the viscoelastic behaviors of polystyrene/multi-walled carbon nanotube (MWCNT) composites during short-term creep and recovery under tensile cyclic loading. Both unmodified and ozone oxidized MWCNTs were applied. It was found in general that the creep strain of thermoplastics dropped with decreasing temperature and stress, and with increasing content of carbon nanotubes. Moreover, with the increased cycle number, the creep strain reduced remarkably. This trend would be even more obvious at high levels of stress and temperature. Further mechanism analysis indicated the network-like structure formed by the molecule chains and nanotubes caused the reduction of the creep strain, the increasing of recovery ratio and the restriction on the mobility of amorphous molecule chains.

1. Introduction

Carbon nanotubes (CNTs) composites have gained enormous attention in research and industrial applications due to their remarkable mechanical, thermal, and electrical properties. The high aspect ratio of CNTs allows property enhancement at lower concentrations as compared with conventional particles such as carbon black or nanoclays [1–6]. To date, Polystyrene (PS) can be found in all the fields in daily life and in the industry production as commonly used plastic material [7–10]. What is more, CNTs reinforced PS matrix composites have been recently studied in a few investigations. Andrews et al. [11] produced PS/MWCNT nanocomposites via melt mixing and reported a small increase in elastic modulus and decrease in tensile strength at low nanotube loading, but as the concentration increased, there were progressive increases in both strength and stiffness. McClory et al. [12] investigated the influence of screw speeds on the electrical and rheological properties of PS/MWCNT composites prepared by a twin-screw extruder. Yuan et al. [13] prepared PS/MWCNT composites by melt-mixing on a kilogram scale using industrial large-scale polymer manufacturing machines like twin-screw extruder and injection molding machine. The mechanical property of the composites was reported when incorporated with MWCNTs in this study. Liao and Li [14] reported a study on the interfacial characteristics of a carbon nanotube reinforced polystyrene composite system through molecular mechanics simulations and elasticity calculations. In the absence of atomic bonding between the reinforcement and the matrix material, it was found that the nonbond interactions consisted of the electrostatic and van der Waals interaction, the deformation induced by these forces, as well as the stress/deformation arising from mismatch in the coefficients of thermal expansion.

In the real case during usage, polymer materials are frequently subjected to different stresses for a period of time. The materials are commonly placed under a load for a long duration, or the stress is repeatedly applied in a working environment. Therefore, the mechanical response, notably the instantaneous and time-dependent deformation is significant for material applications which require dimensional stability. It is the crucial factor that affects the lift time of thermoplastic in an integrated system. Creep test is an essential method to obtain information about the material deformation and mechanical properties like these [15–18]. Yang et al. found that with only 1 vol.% of multi-carbon nanotubes, creep resistance of polypropylene could be significantly improved with reduced creep deformation and creep rate at a long-term loading period [19]. What is more, the creep strain and creep rate of TiO_2 nanoparticles filled polypropylene could be reduced by 46% and 80%, respectively, compared to those of the neat matrix [20]. Several simulation methods have been established to analysis the

* Corresponding authors. Address: National Center for Nanoscience and Technology, Beijing 100190, China. Tel./fax: +86 10 82545586 (Z. Zhang), tel./fax: +86 0551 3600419 (X. Gong).
E-mail addresses: gongxl@ustc.edu.cn (X. Gong), zhong.zhang@nanoctr.cn (Z. Zhang).

1359-835X/$ - see front matter © 2012 Elsevier Ltd. All rights reserved.
http://dx.doi.org/10.1016/j.compositesa.2012.04.011

creep data. Barai and Weng [21–24], for instance, developed several composite models to study the viscoplastic behavior of nanocrystalline materials, including a three-phase composite model to describe the creep behavior. It can be obtained that there existed a critical grain size corresponding to the maximum creep resistance observed, and the critical value varied with the amount of softening pores presented within the solid. Al-Haik et al. [25–27] used high temperature instrumented indentation testing to evaluate the mechanical properties of nanocomposite system. Models such as neural networks model and nonlinear viscoelastic constitutive model were developed to investigate the creep behavior.

However, limited knowledge is known about the recovery behavior of nanoparticle-filled polymers [28,29] when the applied loading is removed, even less about such behaviors under cyclic loading. Muenstedt et al. [30] found the recoverable shear creep compliance became smaller with decreasing nanoclay content under constant load. In our previous work [31], it was observed that incorporation of nanotubes remarkably improved the creep and recovery property of polypropylene. The time–temperature-superposition principle, Weibull distribution function and Burger's models were employed to illustrate relevant strengthening mechanism involved in polypropylene/MWCNTs composites. However, all the studies of creep and recovery mentioned above were conducted under a constant stress rather than under the configuration with multi-loading/unloading cycles with tension. It is noteworthy that materials subjected to cyclic loading can succumb to failure at stress levels much lower than those in static cases, and the destruction process under cyclic stress is different from it under the static ones.

In this paper, the creep and recovery behaviors of PS/MWCNT nanocomposites with various contents of nanotubes were investigated under different stress loads and cycle numbers. The influence of nanotubes on the viscoelastic behaviors in different creep cycles was also analyzed in order to explore the possible mechanisms of observed enhancement of creep and recovery properties.

2. Experimental details

2.1. Materials and preparation of composites

A commercial PS (666D, Sinopec) was used as the base polymer. Multi-walled carbon nanotubes (MWCNTs), as the fillers, were supplied by Bayer MaterialScience AG. According to the information provided by the supplier, the diameter of MWCNTs ranges within 10–20 nm and the length ranges within 1–10 μm. The purity of the MWCNTs is higher than 95%. To improve the dispersion situation of nanotubes when mixed with the matrix, surface modified multi-walled carbon nanotubes (denoted as m-MWCNTs in this paper) were also considered as additional filler. The MWCNTs were functionalized with ozone at room temperature for 2 h as the progress has been discussed in our recent work [32]. PS/MWCNT and PS/m-MWCNT composites were prepared by a two-step melt-mixing strategy to improve the dispersion of fillers. In the first step, the masterbatch with 8.4 vol.% of MWCNTs in PS was prepared in a twin-screw extruder (Haake PTW16, Thermo Fisher, Germany) operating at 220 °C at 80 rpm. In the second step, the PS/MWCNT master batch was diluted to obtain target proportion of 0.6, 1.7 and 2.8 vol.%. After cooling, the extruder blanks were cut as granules with length in a range of 3–5 mm for further preparation of testing samples.

2.2. Characterization and testing

The dispersion status of MWCNTs in the PS nanocomposites was studied by inspecting the fracture surface of the specimens through the scanning electron microscope (SEM, HITAHI S-4800, Japan). The surfaces were gold coated prior to SEM performed at 6 kV acceleration voltage. Inspection was also carried out with transmission electron microscopy (TEM, Tecnai $G^2$20 S-TWIN, FEI, USA) at an acceleration voltage of 200 kV. For investigations of the bulk morphology of samples, thin sections were cut from the PS/MWCNT composites using an ultramicrotome (LKB Nova) with diamond knife.

In order to observe the interface between the PS matrix and nanotubes, the Raman spectra were obtained by using a Renishaw 2000 MicroRaman spectrometer (Reinshaw, Wotton-under-Edge, UK) with an excitation length of 633 nm. The compressive stresses were generated within the MWCNTs by quenching the composite specimen down to specific temperature using the cooling cell. The temperatures used in our experiment ranged from 60 °C down to −60 °C, with a cooling rate of 10 °C/min. Thermal equilibrium was ensured in all the cases by maintaining the specimen under constant temperature for 10 min.

Tensile test of the specimens was carried out with a SANS CMT2000 tester. The granulated materials were injection molded into standard dumbbell-shaped specimens ($30 \times 3.1 \times 3.3$ mm^3, length × width × thickness, according to the ASTM D638 standard) by an injection molding machine (HAAKE MiniJet) for tensile tests. The tests were carried out at a cross head speed of 2 mm/min. Measurements were performed at room temperature with an electrical extensometer whose gauge length was 10 mm. At least five specimens of each composition were tested and the average values were reported.

The creep and recovery tests of PS and nanocomposites were performed by using a dynamic mechanical analyzer (TA Instruments Q800). The time-dependent deformation was measured. The samples for creep and recovery tests were molded with a compression machine at 200 °C and 20 MPa and the specimens' dimensions were 13 mm × 4.3 mm × 0.4 mm (length × width × thickness). The specimens were mounted carefully in a tensile configuration fixture and aligned to avoid any twisting or buckling of the specimens. The applied creep stress was 3, 5 and 8 MPa for a creep time of 600 s followed by a recovery time of 1200 s. The creep–recovery cycle was sequentially repeated two more times. These three-cycle creep–recovery experiment series were performed at two different temperatures of 35 °C and 90 °C.

The typical creep–recovery curve of creep tests performed in a tensile configuration was illustrated in Fig. 1 [33]. Creep strain in the viscoelastic range can be described by the following formula:

$$\varepsilon_c(t) = \varepsilon_E + \varepsilon_V + \varepsilon_\infty \quad (1)$$

here ε_E is the elastic creep strain, ε_V is the viscoelastic portion of the strain and ε_∞ is the permanent creep strain. In the following

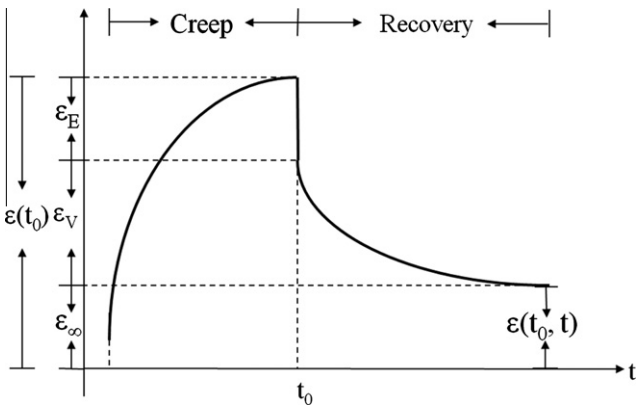

Fig. 1. Schematic diagram of a creep–recovery test.

creep–recovery experiment, the shear stress τ_0 is set to zero at t_0, and the unrecovered strain $\varepsilon(t_0,t)$ is measured. For a given prior stress imposed during the creep period, ε_r is a function of the creep duration t_0 and the recovery time t after that. Thus $\varepsilon_r = \varepsilon_r(t_0,t)$. The recoverable strain ε_r at time t is defined as:

$$\varepsilon_r(t_0,t) = \varepsilon(t_0) - \varepsilon(t_0,t) \quad (2)$$

In order to further analyze the influence of the stress cycles and carbon nanotubes on the recovery performance, the recovery ratio of a system at the time of t is defined as:

$$X_R(t) = [\varepsilon_r(t_0,t)/\varepsilon(t_0)] \times 100\% \quad (3)$$

3. Results and discussion

3.1. Morphology of the nanocomposites

As is known, the homogeneous dispersion of nanotubes in polymer matrices is one of the key factors for making high performance composites. The dispersion was investigated by SEM and TEM in this study. Fig. 2a and b are the SEM images of the fracture surfaces of PS/MWCNT composites with the content of 0.6 vol.% and 2.8 vol.%, respectively. The fracture surface of the PS/MWCNT composite was perpendicular to the injection direction. In order to characterize the state of dispersion, a low magnification was selected. Only small clusters of nanotubes were observed, which indicated that the nanotubes were well distributed in the PS matrix.

TEM observation of a thin section is also a common method utilized to investigate the nanotube dispersion in polymer matrices. The nanotube dispersion state on the plane was observed as illustrated in Fig. 2c. The nanotubes were well dispersed in PS/MWCNT composites (1.7 vol.%). Meanwhile, nanotubes with different forms, such as straight, curved and bundled tubes, caused by thermal and torsion actions during melt extruding process can be found in the image.

3.2. Mechanical properties

As the fundamental properties, the tensile properties of the materials at room temperature have been determined firstly. Fig. 3 shows the key mechanical properties of PS and PS/MWCNTs nanocomposites. The Young's modulus and tensile strength for the neat PS were about 3.3 Gpa and 38.6 MPa. The Young's modulus of the nanocomposites was higher than it of the pure PS. It indicates that the increasing elasticity of nanocomposites is obtained. The elastic properties of PS and PS/MWCNTs composites will be further discussed based on the following creep and recovery measurements. Fig. 3b shows the tensile strength changes with contents of nanotubes. It can be seen that the tensile strengths of pure PS and nanocomposites have no significant variation.

3.3. Creep and recovery behavior of nanocomposites

3.3.1. Stress dependence

The creep and recovery behaviors of the nanocomposites with various contents were investigated under different loads. The resulting PS and PS/MWCNT creep profiles with stress ranging from 3 to 8 MPa at the temperature of 35 °C are presented in Fig. 4. It can be seen that the materials showed different responses to stress levels. The traces of the creep and unrecovered strains as a function of time for pure PS are presented in Fig. 4a. The creep strain and unrecovered creep strain increased distinctly with the increasing stress. During the first cycle for the pure PS, the strain increased from average value of 0.15–0.25% when stress increased from 3 MPa to 5 MPa. The ratio of increasing was about 1:1, but this ratio went up tremendously for the 8 MPa case. It seems to indicate that the material may obtain high level of strain and even get failure much faster under high stress. At the same time, it was

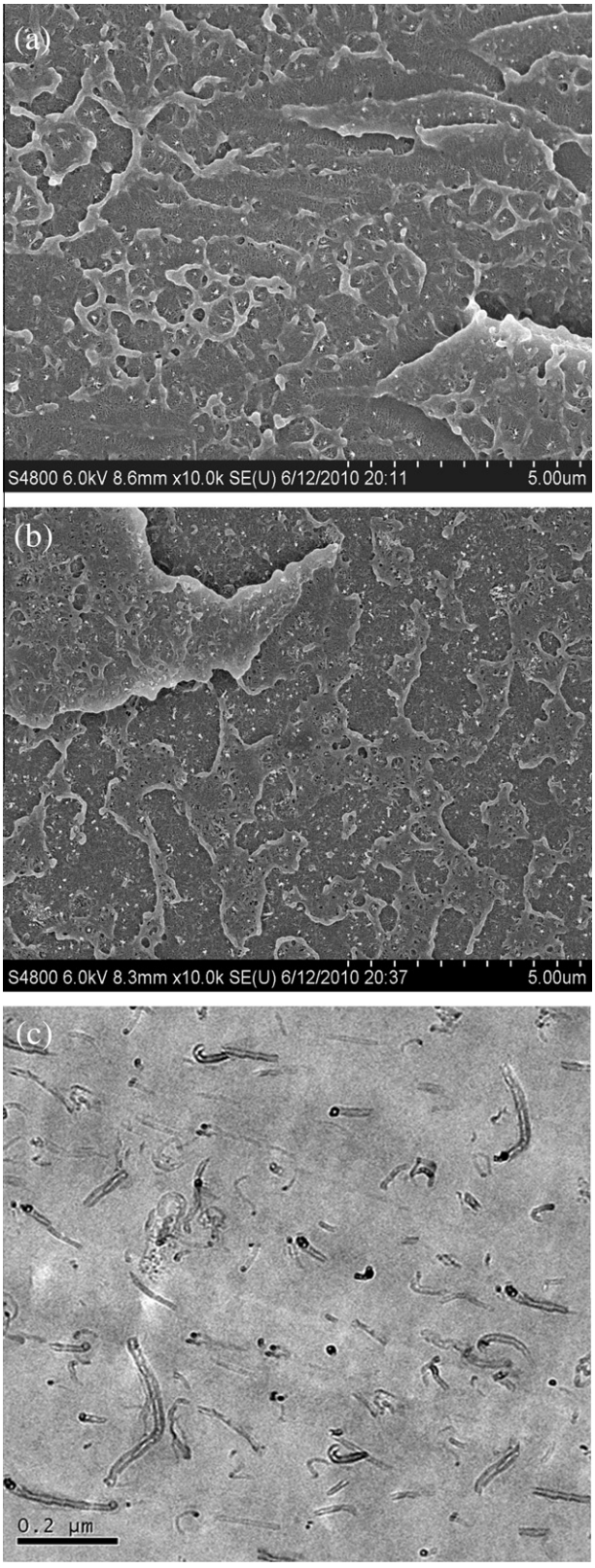

Fig. 2. SEM micrographs of PS/MWCNT nanocomposites with filler content of (a) 0.6 vol.%, (b) 2.8 vol.% and (c) is the TEM micrograph of nanocomposite with filler content of 1.7 vol.%.

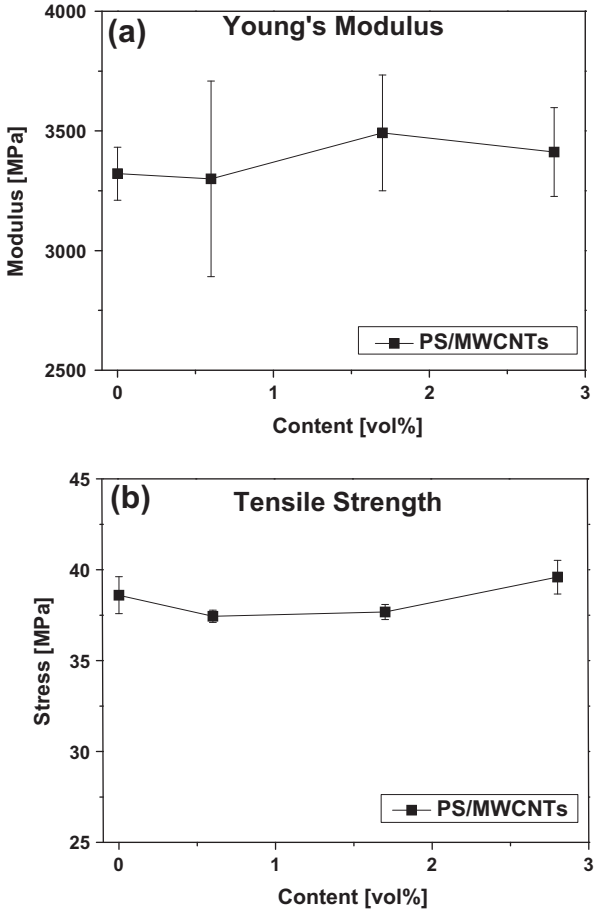

Fig. 3. Tensile mechanical characteristics: (a) Young's modulus and (b) tensile strength of PS and PS/MWCNT nanocomposites with different MWCNT contents.

found that higher imposed stresses resulted in lower recovery ratio X_R as listed in Table 1. For PS, after the single cycle, the recovery ratio $X_R(t = 1800\ s)$ was 88.4% with the stress of 3 MPa and it decreased to 58.4% with the stress of 8 MPa. The results show that high stress level can bring large permanent creep strain and accelerate the final destruction of polymer materials. It indicates the creep and recovery properties of PS have the significant dependence on the stress. Creep mechanism is further explored from the perspective of molecular motion to analysis the stress influence on creep and recovery behavior. In general, the macroscopic viscoelastic properties are closely related with the microcosmic movement of molecular chains or segments. When the polymer materials are resisted in a single directional external force, the molecular chains or segments will be activated and several molecular chain movements occur simultaneously. The first category of movements is the change of the bond lengths and angles in the interior of the polymer chains. When the stress is removed, this change in the molecular chain can recover immediately to the original state. The second category of movements is the extension of molecular chains or segments, which is associated with the relaxation time of the materials. This part of the deformation can be gradually restored over time when unloading. The third category of movements is the relative slippage of molecular chains. After the removal of external loading, these slippages are very difficult to return to the original position thus the deformation is permanent. Comparing the results (in Fig. 4) under different stress conditions, it can be found that for higher stress applying on the material, there will be greater influence on the movements of molecular chains, especially on the extension and slippage of

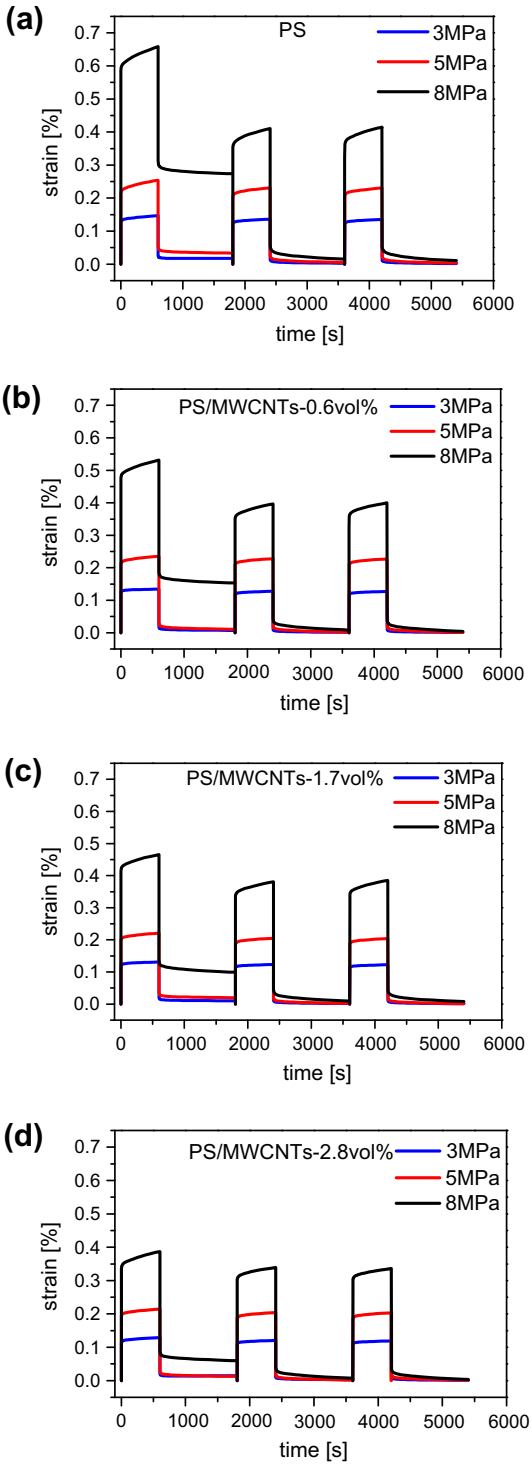

Fig. 4. Creep–recovery curves of PS and PS/MWCNT nanocomposites as a function of time at 35 °C: (a) 0 vol.%, (b) 0.6 vol.%, (c) 1.7 vol.% and (d) 2.8 vol.%.

polymer chains. Hence the high creep stress can accelerate the occurrence of the creep deformation and damage of polymer materials. The same results can be obtained from Fig. 4b–d of PS/MWCNT nanocomposites containing 0.6, 1.7 and 2.8 vol.% MWCNT. Therefore, the composites have the similar dependence on stress as neat PS. It should also be pointed out that X_R with the increasing content of MWCNTs in the first creep cycle has a rising tendency which changes from 58.4% to 84.8% at 8 MPa. The phenomenon and mechanism of the improvement in creep and recovery performance caused by MWCNTs fillers will be discussed in Section 3.3.3.

Table 1
Creep strain, unrecovered strain and recovery ratio for PS and PS/MWCNT composites at 35 °C under different loads.

Volume fraction (%)	Cycle	Creep strain (%)		
		3 MPa	5 MPa	8 MPa
0	1	0.147	0.254	0.659
	2	0.136	0.231	0.411
	3	0.135	0.230	0.411
0.6	1	0.134	0.236	0.532
	2	0.128	0.228	0.396
	3	0.127	0.227	0.401
1.7	1	0.130	0.221	0.465
	2	0.123	0.205	0.381
	3	0.122	0.204	0.381
2.8	1	0.129	0.214	0.387
	2	0.121	0.204	0.339
	3	0.119	0.203	0.336
		Unrecovered strain (%)		
		3 MPa	5 MPa	8 MPa
0	1	0.017	0.033	0.274
	2	0.003	0.005	0.015
	3	0.002	0.003	0.011
0.6	1	0.007	0.010	0.153
	2	0.002	0.002	0.008
	3	0.001	0.001	0.004
1.7	1	0.010	0.020	0.099
	2	0.002	0.002	0.009
	3	0.001	0.001	0.008
2.8	1	0.015	0.013	0.059
	2	0.003	0.002	0.007
	3	0.001	0.001	0.003
		Recovery ratio (%)		
		3 MPa	5 MPa	8 MPa
0	1	88.4	87.0	58.4
	2	97.8	97.8	96.4
	3	98.5	98.7	97.3
0.6	1	94.8	95.8	71.2
	2	98.4	99.1	98.0
	3	99.2	99.6	99.0
1.7	1	92.3	91.0	78.7
	2	98.4	99.0	97.6
	3	99.2	99.5	98.0
2.8	1	88.4	93.9	84.8
	2	97.5	99.0	97.9
	3	99.2	99.5	99.1

3.3.2. Influence of creep cycles

Creep cycles, as an important factor for the creep and recovery properties, are analyzed in this section. As shown in Fig. 4a, the curves of the creep part show similar shape in all three cycles under the stresses of 3 MPa and 5 MPa for pure PS. However, when the stress rose to 8 MPa, the creep strain can be observed to have a significantly decrease with sequential cycles, which reveals that the influence of the numbers of cycles to creep resistance is related to the stress level. When the stress increases, it is considered that a strong stretch should be conducted on materials and a stable structure formed by the molecular chains appears. Applied to a certain external load, the molecular chains through stretching, sliding and overlapping can form the stabilized polymer structure, which is more orderly and elastic than the one before loading. While this structure is subjected to external stress again, it can resist the fractional creep deformation of the polymer material, especially the irreversible part of deformation. Therefore, the unrecovered strain accumulated over three consecutive cycles, with most of the permanent deformation occurring in the first cycle.

The influence of creep cycles was also investigated under a higher temperature condition of 90 °C. Fig. 5 presents the resulting creep and recovery profile over three cycles with creep stress of 5 MPa. It can be seen that Fig. 5 shows obvious difference with Fig. 4. The creep strains under higher temperature were very large, and the materials tended to fatigue. This phenomenon is related to the relaxation of polymer molecular chains under the high temperature. The materials at 90 °C are in the different mechanical state as the ones at 35 °C. Under the higher temperature conditions, the materials were more easily to deform as they were in the glass–rubber region with the high mobility and large relaxation of polymer chains. However, the polymer materials were in the glass region at 35 °C. The mobility of the molecular chains was restricted at the low temperature condition, so the creep strain is small. Moreover, one can recognize from Fig. 5 that with the increase of cycle numbers, the creep strain and unrecovered strain showed an obvious decreasing trend. As listed in Table 2, the creep strain of PS dropped from 3.42% to 2.08% and the unrecovered strain dropped from 2.69% to 1.32%. At the same time, the recovery ratio increased along with sequential cycles as shown. For example, after three cycles, the recovery ratio of pure PS was 36.5%, an increasing of almost 71% of the original value after the first creep cycle. By comparison, it can be seen that with the increasing creep cycle numbers, the change of creep and recovery responses stronger at higher temperature condition. This phenomenon is related to the enhanced mobility of molecular chains. Due to the high temperature, the stretching, sliding and overlapping of chains or chain segments are intensified under single directional tensile force, so it can result in the reducing of creep strain, the rising of recovery ratio and a more stable structure of molecular chains with the applied cyclic stress of repeated loading and unloading. Nevertheless, under the lower temperature condition, the immobility of molecular chains prevents the internal molecular structure stabilized after the first creep cycle as shown in Fig. 4, in which the creep–recovery curves seem to have similar shape in the last two creep cycles at 35 °C. Thus, the influence of creep cycles is more obviously at the high temperature condition than at the low one.

3.3.3. The reinforcement role of MWCNTs in nanocomposites

The results shown in Fig. 4 indicated that creep strains of nanocomposites were lower than those of the neat matrix under all test stresses. This implies that the creep behavior is improved by the presence of nanotubes. One can recognize that the creep strain decreased remarkably with the incorporation of MWCNT under the higher stress. Under the stress of 8 MPa, for instance, the strain values of PS/MWCNT containing 0.6 vol.%, 1.7 vol.% and 2.8 vol.% were reduced by 19%, 29% and 41% compared to that of PS for the first cycle. With regard to the recovery properties of three creep cycles, the added nanotubes can certainly reduce the irreversible creep strain ε_∞ and increase the recovery ratio X_R as shown in Table 1. The ability of nanotubes to restrain the deformation has association with

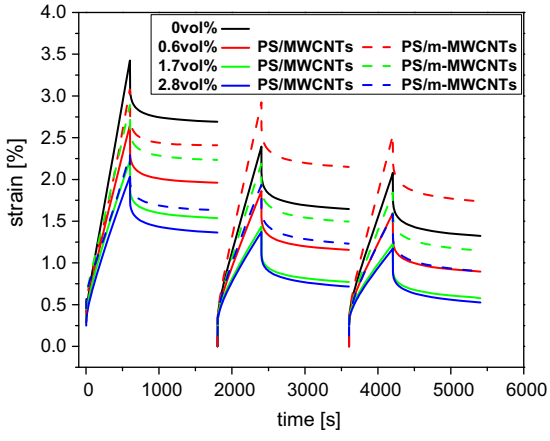

Fig. 5. Creep–recovery curves of PS, PS/MWCNT (solid lines) and PS/m-MWCNT (dashed lines) nanocomposites as a function of time at 90 °C.

Table 2
Creep strain, unrecovered strain and recovery ratio for PS and PS/MWCNT composites at 90 °C.

Volume fraction (%)	Cycle	Creep strain (%)	Unrecovered strain (%)	Recovery ratio (%)
0	1	3.42	2.69	21.3
	2	2.39	1.65	31.0
	3	2.08	1.32	36.5
0.6	1	2.65	1.96	26.0
	2	1.86	1.16	27.6
	3	1.60	0.90	43.7
1.7	1	2.22	1.54	30.6
	2	1.44	0.77	46.5
	3	1.23	0.58	52.8
2.8	1	2.03	1.36	33.0
	2	1.37	0.72	47.4
	3	1.17	0.53	54.7

the network-like structure formed by the molecule chains and nanotubes.

As mentioned, adding nanotubes into PS can certainly affect the creep and recovery behaviors, particularly in the high temperature condition as shown in Fig. 5. Around the glass transition region, molecular motion and rearrangement mechanisms can occur drastically while the material is under tension. In the temperature region of 90 °C, adding nanotubes to polymer matrix can restrain the mobility of the molecular chains by a wide margin. As shown in Table 2, the creep and uncovered strains of the composite with content of 2.8 vol.% MWCNT decrease by 41% and 49%, respectively during the first cycle compared to that of the pure PS. In general the creep and recovery properties are enhanced with increasing content of carbon nanotubes. The creep strain of the composite with the carbon nanotube content of 2.8 vol.% MWCNT is 2.03%, 1.37%, and 1.17% in three creep cycles, which is lower than the creep strain (2.65%, 1.86% and 1.60%) of the composite of 0.6 vol.% MWCNT. Meanwhile, with the increasing content of carbon nanotubes, the unrecovered creep strain is decreased and the recovery ratio is increased. Moreover, enhancement effect of carbon nanotubes in polymer composites increases with the creep sequential cycles. After all three cycles, the recovery ratio $X_R(t = 3600\ s)$ of composites containing 0.6, 1.7 and 2.8 vol.% MWCNT was 43.7%, 52.8% and 54.7%, compared to 36.5% of pure PS.

In Fig. 6, a schematic deformation model of PS/MWCNT composite under uniaxial stress is demonstrated to illustrate the creep and recovery mechanism affected by the existence of nanotubes. As represented in Fig. 6a, MWCNTs are uniformly dispersed in PS without direction before applied to the stress. Under the tensile stress Fig. 6b, the molecule chains and nanotubes become increasingly strained from the original state and aligned with the direction of the stress. What is more, the network-like structure formed by the molecule chains and nanotubes appears due to the applied loading. When tensile stress is removed, as depicted in Fig. 6c, the recovery of PS/MWCNT composite begins, and the relaxation of the network-like structure built by carbon nanotubes and molecule chains starts as well. However, the integrity of the network-like structure is much better than it shown in Fig. 6a before the stress is applied. Compared to the disordered structure before stretching, this network-like structure has the property of elasticity and the strength enhancing effect. With sequential cycles, the composites become more strained from the original state and aligned with the direction of the stress. Therefore, the creep strain occurred in consecutive cycles was reduced. MWCNTs and entangled chain segments form a more orderly network after the first creep cycle, thus the network-like structure can effectively prevent the slippage of molecules. At the same time, the unrecovered strain accumulates over the three consecutive cycles, with most of its portion contributed by the unrecovered deformation occurred in the first creep cycle when no network-like structure forms. The unrecovered creep, or permanent set, is due to the molecular slippage in the amorphous region. This considerable permanent strain is particularly significant in the engineering application as an undesirable material property in most cases. With the highest temperature and stress imposed, it is notably observed that the network-like structure could be more regular after consecutive cycles.

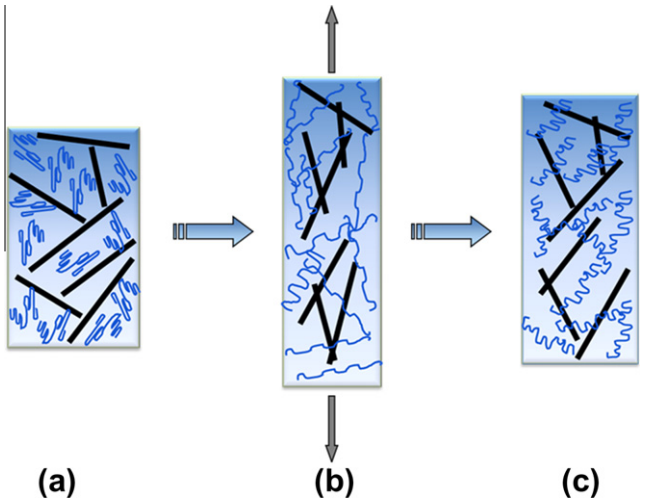

Fig. 6. Schematic deformation model of PS/MWCNT composite under uniaxial stress: (a) before loading, (b) loading, (c) unloading.

In Fig. 5, the creep and recovery properties of PS/m-MWCNT composites were investigated in the same way as PS/MWCNT composites. The results indicate that adding both MWCNTs and m-MWCNTs to the PS matrix can increase the creep resistance and creep–recovery property. Based on the observation, however, it becomes clear that the properties of PS/MWCNT composites are better than PS/m-MWCNT ones. Strong interface is the important factor for MWCNTs reinforced composite, because the external stresses applied to the composite as a whole can be efficiently transferred to the MWCNTs, allowing them to take a disproportionate share of the load. Raman spectroscopy has been widely used to evaluate the interaction between polymers and MWCNTs in composites due to its sensitivity to the interatomic distance. Generally, the interaction between nanotubes and matrix can be reflected by the Raman shifts of the characteristic peaks. By cooling the specimens from 60 °C to −60 °C, the upward shifts of Raman band peak position for PS/MWCNT and PS/m-MWCNT composites were observed in Fig. 7a. As shown in Fig. 7b, the cooling of the embedded materials from 60 °C down to −60 °C caused 12 and 7 cm^{-1} shift for MWCNTs and m-MWCNTs, respectively. Comparing with m-MWCNT filled composite, the MWCNTs embedded in

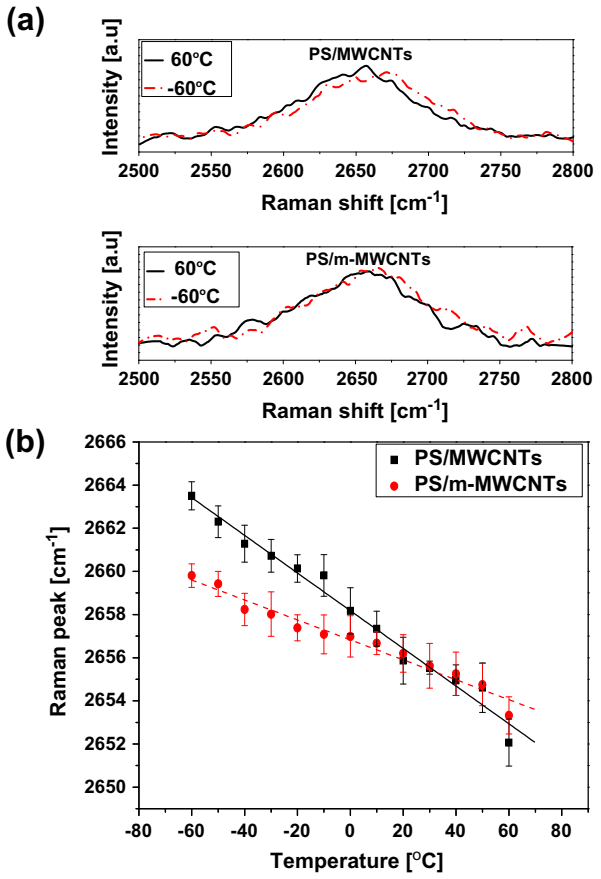

Fig. 7. Typical G′-band Raman spectra: (a) comparison of the Raman spectra for PS/MWCNT and PS/m-MWCNT composites and (b) the Raman shift of G′-band as a function of temperature.

PS matrix shows larger G′-band shift over the temperature range we studied, indicating more efficient load transfer between the MWCNTs and the PS matrix. Therefore, compared to the nanotubes with surface functionalization, MWCNTs without ozone oxidation shows much better load transfer effect in PS matrix. The weak interface condition for m-MWCNTs may due to the different polarity between it and polymer chains. After ozone oxidation, the surface of nanotubes picks up some oxygenic polar groups such as carbonyl [32]. PS, however, is a kind of non-polar hydrophobic polymer, and the polar m-MWCNTs are incompatible with the non-polar polymer chain. Thus the interface performance of m-MWCNTs/PS system is not very good. Similar results were obtained by Barai and Weng [34]. It was shown that MWCNTs were indeed very effective strengthening agents, but imperfect interface condition between MWCNTs and matrix can severely reduce the effective stiffness and elastoplastic strength of the nanocomposite.

4. Conclusions

In summary, this paper studied the creep and recovery behavior of PS/MWCNT nanocomposites under cyclic tensile stress. The creep strain increased with the increase of temperature and stress and decreased with the increase of the content of carbon nanotubes, which indicates an enhanced creep performance at short time scales. The results also indicated that the incorporation of nanotubes decreased the creep strain and unrecovered strain remarkably at higher temperature and stress conditions. Furthermore, the creep and recovery behaviors in different creep cycles were analyzed and the mechanism of observed enhancement was explored. It is believed that the network-like structure formed by the molecule chains and nanotubes can reduce the creep strain, increase the recovery ratio and restrict the molecular slippage in repeat loading cases.

Acknowledgements

This project was jointly supported by the National Nature Science Foundation of China (Grant No. 51073044), a key international collaboration project (Grant No. 2011DFR50200) of the Ministry of Science and Technology of China, and a key item of the Knowledge Innovation Project of the Chinese Academy of Science (Grant No. KJCX2-YW-M20).

References

[1] Iijima S. Helical microtubules of graphitic carbon. Nature 1991;354(6348):56–8.
[2] Suhr J, Victor P, Ci L, Sreekala S, Zhang X, Nalamasu O. Fatigue resistance of aligned carbon nanotube arrays under cyclic compression. Nat Nanotechnol 2007;2(7):417–21.
[3] Suhr J, Koratkar N, Keblinski P, Ajayan P. Viscoelasticity in carbon nanotube composites. Nat Mater 2005;4(2):134–7.
[4] Koval'chuk AA, Shchegolikhin AN, Shevchenko VG, Nedorezova PM, Klyamkina AN, Aladyshev AM. Synthesis and properties of polypropylene/multiwall carbon nanotube composites. Macromolecules 2008;41(9):3149–56.
[5] Wang K, Tang CY, Zhao P, Yang H, Zhang Q, Du RN. Rheological investigations in understanding shear-enhanced crystallization of isotactic poly(propylene)/multi-walled carbon nanotube composites. Macromol Rapid Commun 2007;28(11):1257–64.
[6] Chen GX, Kim HS, Park BH, Yoon JS. Multi-walled carbon nanotubes reinforced nylon 6 composites. Polymer 2006;47(13):4760–7.
[7] Slobodian P, Králová D, Lengálová A, Novotný R, Sáha P. Adaptation of polystyrene/multi-wall carbon nanotube composite properties in respect of its thermal stability. Polym Compos 2010;31(3):452–8.
[8] Carastan DJ, Demarquette NR. Polystyrene/clay nanocomposites. Int Mater Rev 2007;52(6):345–80.
[9] Sun GX, Chen GM, Liu ZP, Chen M. Preparation, crystallization, electrical conductivity and thermal stability of syndiotactic polystyrene/carbon nanotube composites. Carbon 2010;48(5):1434–40.
[10] Bera O, Pilic B, Pavlicevic J, Jovicic M, Hollo B, Szecsenyi KM, et al. Preparation and thermal properties of polystyrene/silica nanocomposites. Thermochim Acta 2011;515(1–2):1–5.
[11] Andrews R, Jacques D, Minot M, Rantell T. Fabrication of carbon multiwall nanotube/polymer composites by shear mixing. Macromol Rapid Commun 2002;287(6):395–403.
[12] McClory C, Potschke P, McNally T. Influence of screw speed on electrical and rheological percolation of melt-mixed high-impact polystyrene/MWCNT nanocomposites. Macromol Rapid Commun 2011;296(1):59–69.
[13] Yuan JM, Fan ZF, Chen XH, Wu ZJ, He LP. Preparation of polystyrene-multiwalled carbon nanotube composites with individual-dispersed nanotubes and strong interfacial adhesion. Polymer 2009;50(14):3285–91.
[14] Liao K, Li S. Interfacial characteristics of a carbon nanotube-polystyrene composite system. Appl Phys Lett 2001;79(25):4225–7.
[15] Ganß M, Satapathy BK, Thunga M, Weidisch R, Pötschke P, Janke A. Temperature dependence of creep behavior of PP-MWNT nanocomposites. Macromol Rapid Commun 2007;28(16):1624–33.
[16] Plaseied A, Fatemi A. Tensile creep and deformation modeling of vinyl ester polymer and its nanocomposite. J Reinf Plast Compos 2009;28(14):1775–88.
[17] Varela-Rizo H, Weisenberger M, Bortz DR, Martin-Gullon I. Fracture toughness and creep performance of PMMA composites containing micro and nanosized carbon filaments. Compos Sci Technol 2010;70(7):1189–95.
[18] Tehrani M, Safdari M, Al-Haik MS. Nanocharacterization of creep behavior of multiwall carbon nanotubes/epoxy nanocomposite. Int J Plast 2011;27(6):887–901.
[19] Yang JL, Zhang Z, Friedrich K, Schlarb A. Creep resistance of polymer nanocomposites reinforced with multi-wall carbon nanotubes. Macromol Rapid Commun 2007;28(8):955–61.
[20] Yang JL, Zhang Z, Friedrich K, Schlarb A. Resistance to time-dependent deformation of nanoparticle/polymer composites. Appl Phys Lett 2007;91:011901.
[21] Barai P, Weng GJ. The competition of grain size and porosity in the viscoplastic response of nanocrystalline solids. Int J Plast 2008;24(8):1380–410.
[22] Barai P, Weng GJ. Mechanics of creep resistance in nanocrystalline solids. Acta Mech 2008;195(1–4):327–48.
[23] Barai P, Weng GJ. Mechanics of very fine-grained nanocrystalline materials with contributions from grain interior, GB zone, and grain-boundary sliding. Int J Plast 2009;25(12):2410–34.
[24] Barai P, Weng GJ. A micro-continuum model for the creep behavior of complex nanocrystalline materials. Int J Eng Sci 2011;49(1):155–74.
[25] Al-Haik M, Garmestani H, Savran A. Explicit and implicit viscoplastic models for polymeric composite. Int J Plast 2004;20(10):1875–907.

[26] Al-Haik M, Hussaini M, Garmestani H. Prediction of nonlinear viscoelastic behavior of polymeric composites using an artificial neural network. Int J Plast 2006;22(7):1367–92.
[27] Tehrani M, Safdari M, Al-Haik M. Nanocharacterization of creep behavior of multiwall carbon nanotubes/epoxy nanocomposite. Int J Plast 2011;27(6):887–901.
[28] Yang JL, Zhang Z, Schlarb AK, Friedrich K. On the characterization of tensile creep resistance of polyamide 66 nanocomposites. Part I: experimental results and general discussions. Polymer 2006;47(8):2791–801.
[29] Yang JL, Zhang Z, Schlarb AK, Friedrich K. On the characterization of tensile creep resistance of polyamide 66 nanocomposites. Part II: modeling and prediction of long-term performance. Polymer 2006;47(19):6745–58.
[30] Muenstedt H, Katsikis N, Kaschta J. Rheological properties of poly(methyl methacrylate)/nanoclay composites as investigated by creep recovery in shear. Macromolecules 2008;41(24):9777–83.
[31] Jia Y, Peng K, Gong XL, Zhang Z. Creep and recovery of polypropylene/carbon nanotube composites. Int J Plast 2011;27(8):1239–51.
[32] Peng K, Liu LQ, Li HC, Meyer H, Zhang Z. Room temperature functionalization of carbon nanotubes using an ozone/water vapor mixture. Carbon 2011;49(1):70–6.
[33] Ward IM. Mechanical properties of solid polymers. Weinheim: John Wiley and Sons Ltd.; 1983.
[34] Barai P, Weng GJ. A theory of plasticity for carbon nanotube reinforced composites. Int J Plast 2011;27(4):539–59.